

Intrinsic Torque and the Global Structure of Self-consistent Intrinsic Rotation Profiles in Flux-Driven ITG Turbulence ¹

S. Ku 1-2), G. Dif-Pradalier 3), S.M. Yi 1), E.S. Yoon 4), P.H. Diamond 1-3), T.S. Hahm 4), W. Solomon 5), C.S. Chang 2), Y. Sarazin 6), V. Grandgirard 6), J. Abiteboul 6), X. Garbet 6), Ph. Ghendrih 6), G. Latu 6), A. Strugarek 6)

1) National Fusion Research Institute, Daejeon, Korea

2) Courant Institute of Mathematical Sciences, New York Univ., New York, USA

3) University of California San Diego, California, USA

4) Princeton Plasma Physics Laboratory, Princeton, New Jersey, USA

5) General Atomics, San Diego, USA

6) CEA/IRF, France

E-mail contact of main author: sku@cims.nyu.edu

Abstract. Global, heat flux-driven gyrokinetic simulations which manifest the formation of macroscopic, mean toroidal flow profiles, with thermal Mach number 0.05, is observed in global ITG simulations. Both PIC (XGC1) and Semi-Lagrangian (GYSELA) approaches are utilized without apriori assumptions of scale-separation between turbulence and mean fields. ITG simulations with no-slip boundary condition using XGC1 and GYSELA show the evolution of intrinsic rotation in the co-current direction. A mean flow is generated to peak with thermal Mach numbers ~ 0.05 . External momentum input can effectively cancel the intrinsic rotation profile. XGC1p results indicate peak intrinsic co-rotation is reduced by a factor of five upon injection of counter directed momentum. Residual stress and intrinsic torque are identified. The probability distribution function of outward heat flux and inward momentum flux show strong similarity. Correlations between residual stress and two symmetry breakers, ExB shear and intensity gradient are similar. A $\rho(\text{star})$ scan of parallel flow values reveals a weak decay of rotation velocity as $\rho(\text{star})$ decreases, and heat source scan shows scaling of intrinsic rotation with heat source. Reversed q gives increased intrinsic rotation.

1. Introduction

Intrinsic rotation is central to ITER performance, since it stabilizes RWM's, may enhance confinement and can affect the L-H transition threshold. Recent experiments uncovered evidence to support the theoretical proposal of an intrinsic, turbulence driven torque density as the drive of intrinsic rotation[1-3]. The momentum flux driven by electrostatic turbulence is mainly given by the Reynolds stress. The Reynolds stress (i.e. radial flux) of toroidal momentum can be decomposed as

$$\Pi_{r,\phi} = -\chi_{\phi} \frac{\partial \langle v_{\phi} \rangle}{\partial r} + V \langle v_{\phi} \rangle + \Pi_{r,\phi}^R,$$

where χ_{ϕ} is the turbulent momentum diffusion coefficient, V is the convective velocity, and $\Pi_{r,\phi}^R$ is the residual stress. Note that the Reynolds stress equals the residual stress when the toroidal flow, $\langle v_{\phi} \rangle$ is zero. In this study, we discuss the residual stress and the intrinsic rotation using numerical simulations.

Most simulation studies of rotation physics focused entirely on the radial flux of toroidal momentum, and did not address actual rotation profile structure and evolution in the presence

of heat flux-driven turbulence. Here, we present global, heat flux-driven gyrokinetic simulations which manifest the formation of macroscopic, mean toroidal flow profiles which are peaked on axis, with peak thermal Mach number $M_T = \langle v_{\parallel} \rangle / v_{Ti} \sim .05$ and which carry a net momentum.

2. Equations and simulation method

In this study, two gyrokinetic turbulence codes, XGC1p (concentric magnetic geometry version of XGC1 [4]) and GYSELA[5] have been used. Both solve 5D gyrokinetic Vlasov equation [6, 7],

$$\frac{\partial f}{\partial t} + \dot{\bar{X}} \cdot \frac{\partial f}{\partial \bar{X}} + \dot{v}_{\parallel} \cdot \frac{\partial f}{\partial v_{\parallel}} = 0,$$

$$\dot{\bar{X}} = \frac{1}{D} \left[v_{\parallel} \hat{b} + \frac{v_{\parallel}^2}{B} \nabla \times \hat{b} + \frac{\mathbf{B} \times (\mu \nabla B - \mathbf{E})}{B^2} \right],$$

$$\dot{v}_{\parallel} = -\frac{1}{D} (\mathbf{B} + v_{\parallel} \nabla \times \hat{b}) \cdot (\mu \nabla B - \mathbf{E}),$$

$$D = 1 + (v_{\parallel} / B) \hat{b} \cdot (\nabla \times \hat{b}),$$

where $f = f(\bar{X}, v_{\parallel}, \mu)$, \bar{X} is the gyro-center position in real space, v_{\parallel} is the parallel velocity, μ is the magnetic moment, \mathbf{B} is the magnetic field, and \mathbf{E} is the gyro-averaged electric field.

Unlike conventional delta-f gyrokinetic codes, which calculate only turbulence perturbation with assumed scale-separation between turbulence and mean profiles, XGC1p and GYSELA solve turbulence and mean field self-consistently by keeping all of the time evolution of f . The numerical approach of XGC1p is particle-in-cell method and that of GYSELA is Semi-Lagrangian. The difference of the underlying numerical schemes of the codes leads to different preference of implementation of boundary conditions. XGC1p enforces a no-slip boundary condition by applying very high friction to parallel flow near the outer boundary,

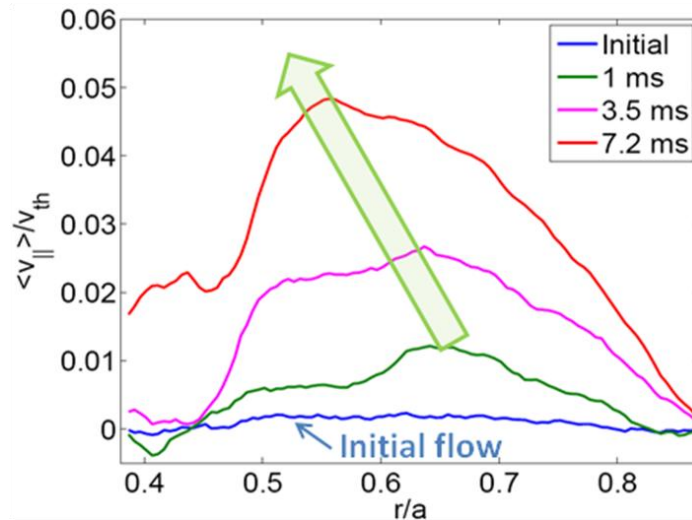


FIG. 1 Generation of intrinsic rotation with no-slip boundary condition using XGC1p. The peak is still increasing and moving inward.

while GYSELA prescribes centered maxwellian on the outer boundary. This no-slip boundary condition is motivated by notions of edge drag by neutral particles. *In this study, the turbulence is flux-driven with heating and cooling of the plasma and the flow speed is zero initially.* Only the ion distribution function is calculated and electrons are assumed to respond adiabatically to the perturbation of ion density. The simulation is performed on the Cray-XT5 machine of National Center for Computational Sciences.

3. Intrinsic rotation and residual stress

FIG. 1 shows the evolution of intrinsic rotation in ITG simulations using XGC1. The simulation started from zero initial flow and near steady state temperature profile. A mean toroidal flow is generated from scratch and achieves peak Mach numbers $M_T \approx 0.05$, in the co-current direction for no-slip boundary conditions. Electrostatic potential Φ_{out} at the outer boundary is held fixed (to zero in the case shown), reflecting edge-physics effects.

In order to explain the origins of intrinsic rotation, an intrinsic torque density – related to $\nabla \cdot \Pi_{r,\phi}^R$ – has been proposed and linked to the structure of the ambient turbulence. The most compelling experimental demonstration of the concept of intrinsic torque is the cancellation experiment of W. Solomon *et al* [1] and K. Ida *et al* [2], in which momentum input against the intrinsic rotation drastically reduces on-axis flow speeds and effectively cancels the intrinsic rotation profile. A stationary plasma is achieved with nearly flat rotation profile, in spite of applied torque. The existence of intrinsic torque density from turbulent residual stress is studied in toroidal geometry under no-slip boundary condition. FIG. 2 shows the corresponding numerical experiment using the XGC1p code with no-slip boundary condition. The safety factor q , the density, and the temperature profiles are adopted from the experiments. ρ_* is 1/298. 1MW heating (cooling) near the magnetic axis (the last closed flux surface) of ion species is applied on the regions of $0.17 < r/a < 0.3$ ($0.78 < r/a < 0.92$), respectively. External torque is applied to cancel the rotation on the region of $0.4 < r/a < 0.8$. Figure 2 shows the initial and the final profiles of parallel flow with and without external

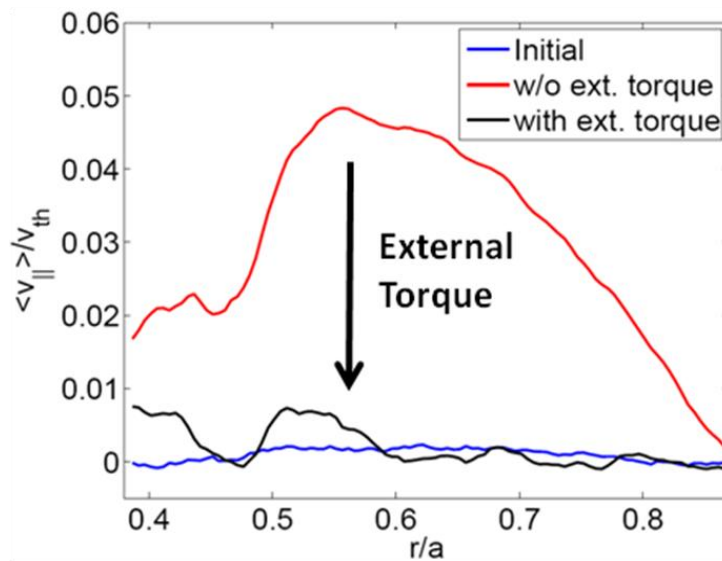


FIG. 2 Initial and final parallel flow of XGC1p simulations with (black) and without (red) external torque canceling the intrinsic rotation.

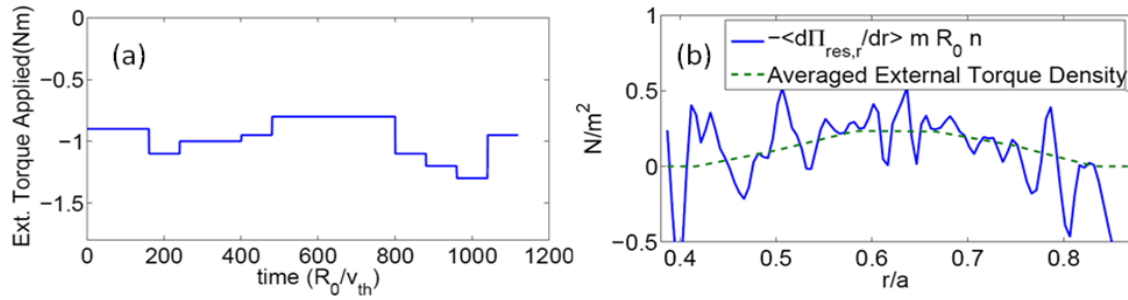


FIG. 3 (a) time history of external torque (b) intrinsic torque and external torque density (the sign is reverted.)

torque. Without external torque, we have observed $M_T \approx 0.05$ of intrinsic rotation after 7 ms ($\cong 1200 R_0 / v_{th}$) from zero initial flow. When we applied the external torque, the local $M_T \approx 0.008$. Note that global cancellation was achieved. These results constitute a clear demonstration-of-principle of the concept of a local, intrinsic torque density and its relation to intrinsic rotation.

The whole simulation consist of tens of short simulations, and at the ends of short simulations the magnitude of torque input and its radial profile were slightly adjusted to avoid excessive or insufficient torque input. About 1 Nm of counter direction torque is applied during the simulation, and the torque from Reynolds stress tracks the external torque input. (FIG. 3) During the simulation the local M_T is maintained to fairly small number. Hence, the torque from residual stress (see FIG. 4) can be interpreted as a residual stress. The residual stress is inward and decreasing towards to edge up to $r/a < 0.8$, and this residual stress gives co-current intrinsic torque. Counter-current torque where $r/a > 0.8$ is disposed of by no-slip boundary condition. In particular, core plasma stresses are transmitted to the boundary turbulent transport (i.e. fluctuation Reynolds stress).

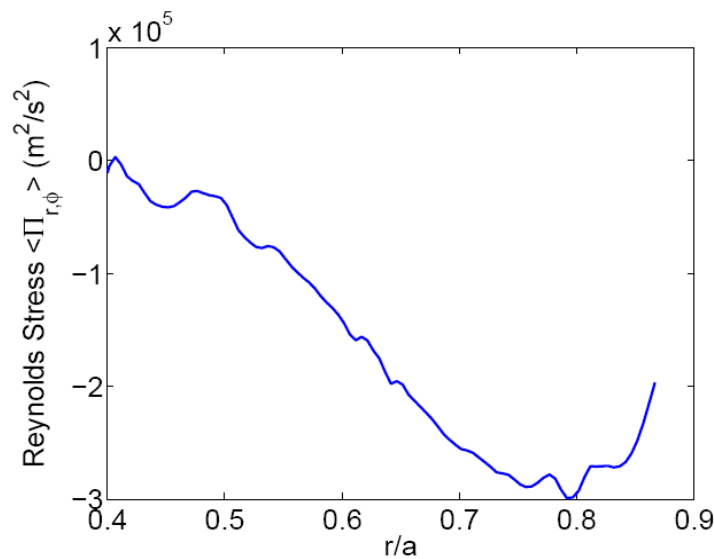


FIG. 4 Reynolds stress obtained in the cancellation simulation using XGC1p. Since toroidal flow is negligible, the Reynolds stress is dominated by Residual stress.

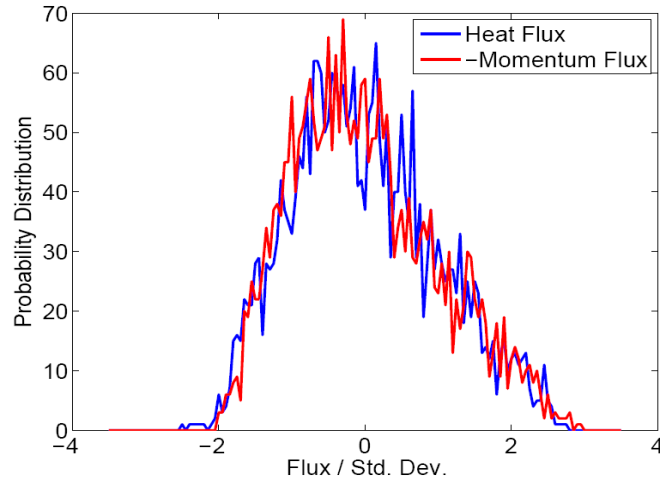


FIG.5 Probability distribution functions of outward heat flux and inward momentum flux. The centers of distribution functions are shifted to zero and they are normalized by standard deviations.

During the simulation, the turbulence arises near the outside boundary and propagates inward as avalanches, and these avalanches drive outward heat flux and inward momentum flux. FIG. 5 shows the probability distribution of outward heat flux and inward momentum flux at $r/a=0.65$. The centers are shifted to zero and x-axis is normalized by standard deviations. Amazingly, they are very similar with each other. The same similarity is observed on the radial positions where significant intrinsic torque exists. This tells us that outward heat avalanches drive inward momentum avalanches, and it is further evidence for non-diffusive, temperature gradient driven nature of momentum flux due to residual stress.

We speculate here that somewhat counter-intuitive findings that core MHD activity appear to enhance intrinsic rotation [8] may be due to the relation between outward heat avalanches and inward momentum avalanches. In particular, the sawtooth crash triggers an outward heat pulse, which in turn results in an inward momentum avalanche, leading to an increase in (intrinsic) rotation.

In this study, we compared two theoretical candidate mechanisms for residual stress, k-parallel symmetry breakings by ExB shear and intensity gradient[9-11]. FIG. 6 shows the correlations between residual stress, divergence of residual stress (intrinsic torque), ExB shear, and divergence of residual stress. Note that the correlations are obtained in Fourier space, and the magnitudes of correlations are shown in the figure. For example, anti-correlation gives 1 instead of -1.

Due to the strong correlation between residual stress and turbulence intensity, intrinsic torque and intensity gradient (which are radial derivatives of residual stress and turbulence intensity) show large correlation with each other. ExB shear also shows a strong (~ 0.6) correlation with intrinsic torque, while it shows slightly smaller (~ 0.4) correlation with residual stress. The correlations of intensity gradient are similar to those of ExB shear, and even larger in some regions. This shows the possible importance of intensity gradient as a major k-parallel symmetry breaking mechanism.

FIG. 7 shows the phase lag between those quantities. Intensity gradient and ExB shear show approximately $\pi/2$ and $-\pi/2$ phase lag relative to residual stress. Phase lag between ExB shear and intensity gradient is about $\pi/2$, too. The phase lag between residual stress and symmetry breakers is consistent with the drift acoustic response of parallel velocity to pressure. In particular, the phase lag between parallel gradient of pressure and parallel velocity is convolved with spectrally averaged k-parallel to form the residual stress. The additional phase lag is likely a consequence of drift-acoustic dynamics.

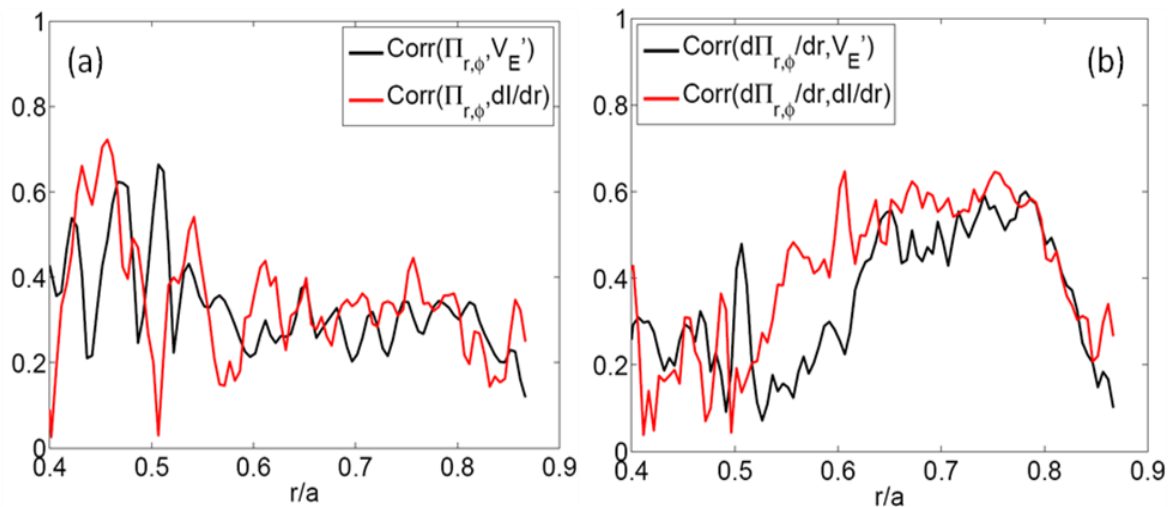


FIG. 6 (a) Correlation between residual stress, and ExB shear and intensity gradient.. (b) Correlation between divergence of residual stress (intrinsic torque), and turbulence ExB shear and intensity gradient.

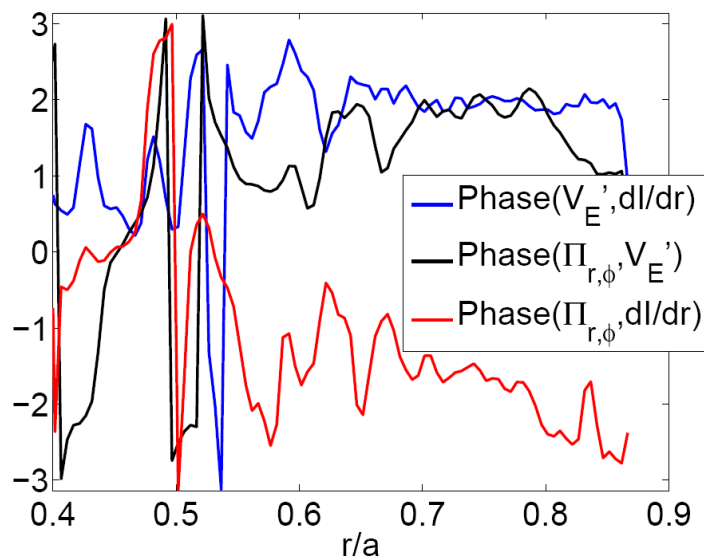


FIG 7 Phase lag between residual stress, intensity gradient, and ExB shear.

We also did some parameter scans of intrinsic rotation. ρ_* scan of intrinsic torque with XGC1p shows very weak decline of intrinsic torque with decrease of ρ_* in qualitative agreement with trends in the database[12]. Here, the measurements of intrinsic torque are from the generation of parallel flow during a short simulation with zero initial flow. Heat source scan with GYSLEA shows increasing intrinsic rotation as heat source increased. Reversed q simulation with GYSELA shows higher toroidal rotation than that for usual q-profiles.

4. Summary

In this study, we have performed flux-driven gyrokinetic simulation with self-consistent turbulence and mean field to understand intrinsic rotation and residual stress. We have used XGC1p and GYSELA with no-slip boundary. Both codes obtained residual stress by applying external torque which cancels the intrinsic rotation. These results constitute a clear demonstration-of-principle of the concept of a local, intrinsic torque density and its relation to intrinsic rotation. Comparison of probability distribution functions of outward heat flux and inward momentum flux shows remarkable similarity. It implies that inward momentum flux avalanches are driven by outward heat flux avalanches. Correlation study shows that intensity gradient is correlated with residual stress and intrinsic torque as much as ExB shear does. Hence, intensity gradient should be considered as important possible symmetry breaker as ExB shear is. A ρ_* scan of parallel flow values reveals a weak decay of rotation velocity as ρ_* decreases, and heat source scan shows scaling of intrinsic rotation with heat source. Reversed q gives increased intrinsic rotation.

References

- [1] W. M. Solomon, K. H. Burrell, A. M. Garofalo, *et al.*, Phys. Plasmas 17, 056108, 2010
- [2] K. Ida, M. Yoshinuma, K. Nagaoka, M. Osakabe, *et al.*, Nucl. Fusion 50, 064007, 2010
- [3] M. Yoshida, Y. Kamada, H. Takenaga, Y. Sakamoto, *et al.*, Phy. Rev. Lett 100, 105002, 2008
- [4] S. Ku, C.S. Chang, P.H. Diamond, Nuclear Fusion, 49, 115021, 2009
- [5] Y. Sarazin, V. Grandgirard, J. Abiteboul, S. Allfrey, *et al.*, Nucl. Fusion, 50, 054004, 2010
- [6] R. G. Littlejohn, Phys. Fluids, 28, 2015, 1985
- [7] T. S. Hahm, Phys. Fluids, 31, 2670, 1988
- [8] S. Coda, and TCV Team “Progress and Scientific Results in the TCV Tokamak”, OV/5-2, 23rd IAEA FEC, Daejeon, Korea, 2010
- [9] Ö. D. Gurcan, *et al.*, Phys. Plasmas 14, 042306, 2007
- [10] Ö. D. Gürcan, P. H. Diamond, P. Hennequin, C. J. McDevitt, X. Garbet, and C. Bourdelle, “Residual parallel reynolds stress due to turbulence intensity gradient in tokamak plasmas”, submitted to Physics of Plasmas, 2010.
- [11] W. X. Wang, T. S. Hahm, S. Ethier, G. Rewoldt, W. W. Lee, W. M. Tang, S. M. Kaye, and P. H. Diamond, Phys. Rev. Lett. 102, 035005, 2009.
- [12] J.E. Rice, A. Ince-Cushman, J.S. deGrassie, L.-G. Eriksson, *et al.*, Nucl. Fusion 47, 1618, 2007